©Copyright 1993 by The Humana Press Inc.
All rights of any nature whatsoever reserved.
0273-2289/93/3940—0491$04.60

Effect of Sugar Consumption on Ethanol Fermentation in a Tower Fermentor Packed with Self-Aggregating Yeast

Mathematical Modeling and Bed Height Prediction

C. S. CHEN, E. CHAN, C. S. GONG, AND L. F. CHEN*

Department of Food Science, Purdue University, West Lafayette, IN 47907

ABSTRACT

A strain of self-aggregating *Saccharomyces uvarum* was cultivated in a 6-L tower fermentor for continuous ethanol fermentation. Large aggregates (2–3 mm) were formed and packed in the column. The height of this packed region depends on the sugar concentration. As sugar concentrations were reduced to below a critical value, most of the large aggregates disintegrated into smaller aggregates (0.1–0.2 mm). Above the packed bed region, small aggregates and small amount of large aggregates were fluidized and formed a well mixed region by the liquid medium and the produced carbon dioxide. A mathematical model of a plug flow with consideration of axial dispersion and a Continuous Stirred Tank Reactor (CSTR) in series is proposed to describe such fermentor. The concentration profile of sugar can be simulated by this model. The height of the packed bed region can then be estimated based on the predetermined critical sugar concentration. Final ethanol concentration and the productivity of such fermentor can also be predicted.

Index Entries: Yeast; aggregates; ethanol fermentation; tower fermentor; model.

*Author to whom all correspondence and reprint requests should be addressed.

INTRODUCTION

Self-aggregating yeast (*Saccharomyces uvarum* U4) has the following advantages over the traditional yeast immobilization system for the production of ethanol in a tower fermentor: higher cell densities (70–100 g dry cell/L) than the immobilized cell system (30–50 g dry cell/L) (*1–5*), highly resistant to contamination caused by high cell density and rapid increase in ethanol concentration, actively growing and self-maintained. The establishment of a packed column is as simple as that of a stirred tank fermentor with no special procedures are required.

Because of the large size (2–3 mm) of the yeast aggregates, this yeast is able to form a packed bed at relatively high medium flow rate. Theoretically, a plug flow reactor is more desirable than a CSTR in terms of volumetric productivity (*6*). In a plug flow fermentor, only the portion of the yeast cells in the down stream experience product (ethanol) inhibition, whereas in a CSTR, all yeast cells are under the same product inhibition. Therefore, it is desirable to establish a packed bed in a tower fermentor with the bed height as high as possible. However, there are limits to bed height for self-aggregating yeast to form a packed bed in the fermentor. One apparent limiting factor comes from the large amount of carbon dioxide generated from fermentation. Carbon dioxide rises to the top of the column at a high flow rate, which ruptures and/or fluidizes the cell aggregates. Small aggregates (<0.3 mm) are formed and fluidized by a high fluid (carbon dioxide and liquid medium) flow rate, thus, a well-mixed region is established at the top of the packed bed region. In previous study (*7*), we have observed the fluidization of cell aggregates when the total superficial velocity of gas (carbon dioxide) and liquid exceeds the minimum fluidization velocity of the cell aggregates. This phenomenon was characterized as hydrodynamic limitation on the height of the packed bed region. Another observation was the reduction in aggregates size when the substrate concentration was reduced and ethanol concentration was increased to certain levels. This phenomenon was characterized as nutrient limitation. Nutrient limitation has been correlated to sugar concentration, i.e., when sugar concentration dropped below a certain value, cell aggregates existed in smaller size (<0.3 mm) and became fluidized (*7*). This critical sugar concentration was found to vary with feed composition and type of sugar, and is independent of dilution rate. However, the location where sugar concentration drops to this critical value is dependent on dilution rate.

For the purpose of reactor design, it is necessary to know the volume of both the packed bed region and the mixed region before the productivity of the fermentor can be predicted. Therefore, it is crucial to be able to predict the height of the packed bed region, thus, the volume of each region can be calculated.

Continuous ethanolic fermentation in a tower fermentor packed with self aggregating yeast has been studied by many researchers in recent years (*1,2,4,5,7–10*) and few of them discussed modeling of such system. Peterson et al. (*19*) used a model for packed bed reactor with axial dispersion to simulate an immobilized yeast tower fermentor by taking into account the effect of carbon dioxide flow rate on the dispersion coefficient. Admassu and Korus (*1*) studied reaction kinetics of converting glucose to ethanol and hydrodynamics in a tower fermentor. A dispersion model that takes axial dispersion into consideration was proposed to describe the packed bed region of the fermentor. In their studies (*1*), the dispersion coefficient was found to be nearly constant throughout the column, which could be a good approximation only at the low carbon dioxide generation rate and low medium flow rate. The mixed region of the fermentor was not accounted for.

In this study, we attempt to include both the packed bed region and the mixed region in our model by assuming this tower fermentor system as a serial connection of a packed bed and a CSTR. The effect of carbon dioxide on the axial dispersion was also taken into consideration. By combining the mathematical model and the experimentally determined limitations on the height of the packed bed region, we are able to estimate the height of the packed bed region, the concentration profile, the volume of the mixed region, and the productivity of the fermentor.

MATERIALS AND METHODS

Materials and Organism

A mutant of *Saccharomyes uvarum* (ATCC 26602) that formed large and stable aggregates was used as biocatalyst (*8*). Sugarcane black strap molassas was supplied from the US Sugar Corporation and Savannah Sugar Foods and Industries. Corn steep liquor and corn dextrose syrup were gifts from A. E. Staley Co., Lafayette, IN.

Seed Culture

Seed culture was grown in 200 mL of molasses growth medium containing 7% (W/V) of sugar and 2% (W/V) of corn steep liquor in a 500-mL flask. The flask with seed culture was incubated in a shaker maintained at temperature of 30°C and at a speed of 150 rpm. After 3 d of incubation, the flask contained about 3 g of wet yeast cells.

Apparatus

Polycarbonate tubing of 6.35-cm od, 5.715-cm id, and 115 cm in length was used to construct the tower fermentor. A cone shape cell

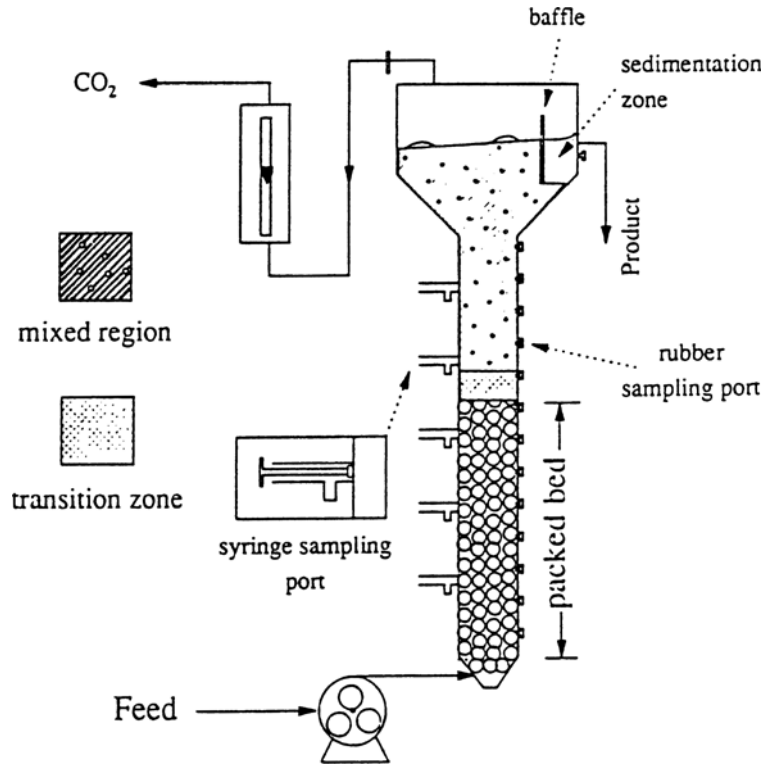

Fig. 1. Diagrammatic configuration of tower fermentor with self-aggregating yeast.

separator, which has a volume of 3.3 L, was attached to the top of the column as shown in Fig. 1. Total working volume of the column was 6.1 L. Sampling ports were constructed from base to the top of column at 5-cm intervals. Fermentation medium was pumped into the column fermentor from the bottom by a peristaltic pump and was overflowed from the cell separator on top of the column fermentor (Fig. 1).

Column Start-Up

Before inoculation, the tower fermentor was sterilized with bleach solution (5% W/V) for 20 min, and then rinsed with 4L of sterilized water. Inoculation was done by pouring the seed culture into the column, and the fresh medium containing 7% (W/V) sugar and 2% (W/V) corn steep liquor was pumped into the bottom of the tower fermentor. The medium flow rates were 100, 400, and 700 mL/h for the first, second, and third d, respectively. After 5 d, the height of the packed bed region increased to a steady level of about 50 cm. Medium containing 12% (W/V) was then pumped into the column. The pH of the medium was about 5 before entering the fermentor, and dropped shortly after entering the fermentor to

about 4.3 and was fairly constant throughout the fermentor. The cell separator contains a baffle (Fig. 1), which separates the uprising carbon dioxide and the outgoing liquid. Cell aggregates were able to fall back into the fermentor in the sedimentation zone (Fig. 1). The cell mass in the fermentor accumulated to a level of about 100 g dry cell/L, after this cell concentration level, further increased cell mass was pushed out of the fermentor by the cell slurry, through the sedimentation zone. The tower fermentor was operated at different flow rates, sugar concentrations, and type of substrate. When flow rate was changed, 12 h of operation was allowed before taking samples. When substrate was changed, 24 h of operation was allowed before taking samples. This is to assure a steady-state operation.

Measurement of Height of Packed Bed

A distinct boundary between two regions (packed bed region and well mixed region) was observed. The height of the packed bed region was measured visually as shown in Fig. 1.

Analytical Methods

Samples were taken periodically from the rubber sampling ports (Fig. 1), which are 5 cm apart. Samples were centrifuged immediately and frozen for later analysis. Sugar concentration was measured by HPLC (Waters Associates, with an Amino-RP column). Ethanol concentration was analyzed by gas chromatography (Varian aerograph 1700).

Cell mass was measured by draining known volume of slury from 5 evenly distributed sampling syringes (1.5 cm ID with side arms of 1.0 cm opening) attached to the fermentor (Fig. 1). Collected slury was centrifuged immediately and oven dried at 60°C for 48 h.

MATHEMATICAL MODELING AND BED HEIGHT PREDICTION

Bed Height Estimation

As mentioned in the Introduction, the bed height can be limited by either low substrate level or fast fluid flow rate. From our previous studies (*7*), the critical substrate level (S_c) at which the nutrient limitation occurs, and the superficial fluid velocity (carbon dioxide + liquid) (Q_c) at which the hydrodynamic limitation occurs, have been estimated (*7*). In order to estimate the bed height at various medium flow rates and/or input substrate concentrations, we simulate the concentration profile of substrate (S) and the flow rate of carbon dioxide (W_{CO_2}) at various axial position (z) by first assuming the reactor as an infinite long packed-bed

column. If substrate concentration decreases to S_c at the axial position z_1, the condition of nutrient limitation appears and the cell aggregates start to disintegrate. In this case, the height of the packed bed region is z_1. On the other hand, if the total superficial fluid velocity at axial position z_2 increases up to Q_c before the substrate concentration drops below S_c, the phenomenon of hydrodynamic limitation occurs and the height of the packed bed region is z_2. The regions of axial position higher than z_1 or z_2, which behave as a continuous stirred tank reactor, was treated separately.

Mathematical Model

In a tower fermentor containing self-aggregating yeast, a distinct boundary between packed bed and well mixed region can be observed (Fig. 1). The packed bed region consisted of large cell aggregates with a diameter of about 2–3 mm and the well mixed region was filled with small cell flocculants with a size smaller than 0.3 mm in diameter. Since the particle size, bed porosity, cell density, and flow pattern are significantly different in these two regions, we simulate the behavior of this tower fermentor as a serial connection of a packed bed reactor and a continuous stirred tank reactor.

Packed Bed Region

A dispersion model was employed to simulate the packed bed region. According to our observations, the flow rate of CO_2 increases tremendously along the column and therefore the axial dispersion coefficient (D_a) is not a constant. Therefore, we adapt the formulation proposed by Peterson et al. (*11*), which considers D_a as a function of the mass flow rate of CO_2 (W_{CO_2}).

Taking axial dispersion into account, a steady state material balance of substrate over a disc element of a column reactor can be expressed as follows:

$$\frac{d}{dz}\left(-D_a\frac{dS}{dz}\right) + \frac{d(u_L S)}{dz} - \eta r_s = 0 \qquad (1)$$

Since a tapered section of 5 cm was used to aid the distribution of nutrient near the entrance, the material balance near the entrance is a little different:

$$D_a\frac{d^2S}{dz^2} + \left(\frac{2D_a\tan(\theta)}{r} + \frac{dD_a}{dz} - u_L\right)\frac{dS}{dz} + \eta r_s = 0 \;;\quad \text{for } z \leq 5\text{cm} \qquad (2)$$

In Eqs. (1) and (2), z represnts the axial position, r_s denotes the rate of substrate consumption, u_L is the superficial velocity of liquid, Θ is the angle between the tapered surface and the axis of the column, and η denotes the effectiveness factor of the cell aggregates. The model proposed by Peterson et al. (*11*) for axial dispersion coefficient is expressed as follows:

$$D_a = D_{ao} + \alpha \left(1 - e^{-\beta W_{co_2}} \right) \quad (3)$$

where D_{aO}, α and β are empirical constants. Since D_a is a function of W_{CO_2}, which increases with increasing axial position z, therefore, D_a is a function of z. The major products are ethanol and carbon dioxide. The concentration of ethanol (p) and the superficial mass flow rate of CO_2 (W_{CO_2}) are calculated as follows:

$$p = Y_{p/s} (S_o - S) \quad (4)$$

$$W_{CO_2} = Y_{CO_2/S} (S_o - S) F \quad (5)$$

Where F in Eq. (4) is the volumetric liquid flow rate.

The above nonlinear ordinary differential equation was solved by a differential equation solver: COLSYS (*12,13*), which uses the spline collocation method to solve mixed order ordinary differential equations. Danckwarts boundary counditions was used at the entrance. The boundary conditions used to solve this equation are stated as follows:

$$@\ z = 0, \qquad \frac{dS}{dz} = \frac{\left(u_L - \frac{2D_a \tan(\theta)}{r}\right)}{D_a} (S_O - S)$$

$$@\ z \rightarrow \infty, \qquad \frac{dS}{dz} = 0$$

We denoted the solution of Eq. (1) with the above boundary conditions as U_∞. To approach this solution numerically for the boundary condition at $z \rightarrow \infty$, we compared the solutions of the following boundary conditions:

$$@\ z = 0, \qquad \frac{dS}{dz} = \frac{\left(u_L - \frac{2D_a \tan(\theta)}{r}\right)}{D_a} (S_O - S)$$

$$@\ z = L, 2L, 3L, \cdots \qquad \frac{dS}{dz} = 0$$

where L is the characteristic length and was taken as 110 cm in our simulation. We denote these solutions as U_j ($j = 1,2,3, \ldots$), which correspond to different boundary conditions. If solution U_n is identical with U_{n-1} at the region $z < L$. The solution U_n (solution of Eq. (1) with boundary condition $dS/dz = 0$ at $z = nL$) was then taken as the approximation of U_∞.

The effectiveness factor was estimated solving an ordinary differential equation that was derived from material balance of the reaction taking place within the biocatalyst in the same way as described by Peterson et al. (*11*):

$$\frac{d}{d\omega}\left(\omega^2 \frac{dS}{d\omega}\right) = - \left(\frac{R^2}{D_{glucose}}\right) \omega^2 r_S \quad (6)$$

with boundary conditions:

$$@\ \omega = 0 \qquad \frac{dS}{d\omega} = 0$$

$$@\ \omega = 1 \qquad S = S_{bulk}$$

Ethanol condition at positions inside the cell aggregates was estimated by:

$$p = p_{bulk} + Y_{P/S}(S_{bulk} - S)\left(\frac{D_{glucose}}{D_{ethanol}}\right) \quad (7)$$

The effectiveness factor was evaluated as follows:

$$\eta = \frac{3D_{glucose}S_o\left(\frac{dS}{d\omega}\right)_{\omega=1}}{\left(R^2 r_S\right)_{S=S_{bulk}}} \quad (8)$$

In Eqs. (6–8), ω is the radial distance from the center of the cell aggregates, $D_{glucose}$ is the effective diffusivity of glucose, $D_{ethanol}$ is that of ethanol, and S_o is the sugar concentration of the feed. Peterson et al. (*11*) used the diffusitivities of glucose and ethanol in water as an approximation of the diffusitivities of glucose and ethanol in the immobilized gel beads. Here, the same approximations were applied on the diffusivities of glucose, fructose, sucrose, and ethanol in the cell aggregates.

Well-Mixed Region

In this region, small cell aggregates (<0.03 mm) were vigorously agitated by uprising carbon dioxide and liquid. This region was described by an ideal CSTR as follows:

$$\begin{aligned} &(S_{in} - S_{out})F = V_{CSTR}\, r_S\, \eta \\ &\text{where } V_{CSTR} = V_{\text{mixed region}}(1 - \varepsilon_g) \\ &\varepsilon_g \text{ is the gas holdup of the mixed region .} \end{aligned} \quad (9)$$

Mersmann's model (*14*) for estimating gas holdup in a slurry bubble column was found to give ϵ_g that's close to measured data in our system and was adopt in the simulation for the mixed region:

$$\frac{\varepsilon_g}{(1-\varepsilon_g)^4} = 0.14U_g\left(\frac{\rho_l^2}{\sigma(\rho_l - \rho_g)g}\right)^{1/4}\left(\frac{\rho_l^2\sigma^3}{\mu_l^4(\rho_l - \rho_g)g}\right)^{1/24}\left(\frac{\rho_l}{\rho_g}\right)^{1/36}\left(\frac{\rho_l}{\rho_l - \rho_g}\right)^{1/3} \quad (10)$$

Where ρ_l and ρ_g are the densities of liquid and gas, σ is the surface tension of the liquid, U_g is the superficial velocity of the gas, and g is the gravitational constant. Surface tension of water was used as an approximation of σ in this equation.

Reaction Kinetics

The rate of substrate consumption is obtained under the following assumptions:

1. The rate of substrate consumption (r_s) is proportional to the rate of ethanol production (r_p). That is:

$$\frac{r_s}{r_{so}} = \frac{r_p}{r_{po}} \tag{11}$$

where r_{so} denotes the maximum substrate consumption rate and r_{po} is the maximum ethanol production rate.

2. The ethanol production rate follows a monod type response to substrate concentration:

$$\frac{r_p}{r_{po}} = \frac{S}{K_S+S} \tag{12}$$

3. The product inhibition follows Luong's formulation (*15*):

$$\text{Product inhibition} \propto \left[1 - \left(\frac{p}{p_m}\right)^{\lambda}\right], \qquad 0 \le p \le p_m \tag{13}$$

where p_m is the maximum ethanol concentration at which cells stop producing ethanol.

4. Ethanol production was found to be inhibited at high sugar concentration. The substrate inhibition is expressed according to conventional type of substrate inhibition (*15*):

$$\text{Substrate inhibition} \propto \frac{K_i}{K_i + S} \tag{14}$$

Combining the above equations, the final form of substrate consumption rate can be expressed as follows:

$$r_S = -r_{So} \frac{S}{K_S+S} \frac{K_i}{K_i+S} \left[1 - \left(\frac{p}{p_m}\right)^{\lambda}\right] x \tag{15}$$

where "x" is the cell density.

RESULTS AND DISCUSSION

Parameter Estimation

The fermentation kinetic constants for both molasses and corn syrup were obtained from batch experiments in the shaker flask. The constants includes K_i, K_S, P_m, r_{so}, and λ in Eq. (15), they were used as an approximation in modeling the tower fermentor. These kinetic constants are comparable to those values in the literature (*1,10,11,15,16*) and are shown in Table 1.

Equation (6) was first solved in order to obtain the relationship between the effectiveness factor and sugar concentration. This relationship was later used in solving Eq. (1). The three hydrodynamic constants (D_a, α, β) were first hand adjusted within realistic ranges to get a converged solution that is close to experimental results. The cell densities at various flow rates and sugar concentrations were measured by taking samples

Table 1
Kinetic and Hydrodynamic Constants for Corn Syrup and Molasses Fermentation

Constant	Unit	Corn syrup	Molasses
r_{so}	g/g-h	3.1	2.0
K_S	% (w/v)	0.052	0.074
K_i	% (w/v)	30.0	23.0
p_m	% (w/v)	12.1	11.0
λ	—	0.78	0.3
D_{ao}	cm^2/h	38	22
α	cm^2/h	4280	3587
β	hr/cm^2 g CO_2	0.072	0.042

Where
r_{So} = maximum ethanol production rate.
K_S = Michaelis constant for ethanol production rate in Eq. (15).
K_i = substrate inhibition constant for ethanol production rate in Eq. (15).
p_m = maximum ethanol concentration for ethanol production.
λ = kinetic constant (the power term) in Eq. (15).
D_{ao} = base value of the dispersion coefficient when no CO_2 is flowing through the column [19].
α = pre-exponential term in calculation of the dispersion coefficient [19].
β = exponential coefficient in calculation of the dispersion coefficient [19].

from syringe sampling ports. All the measurements in the packed bed region gave similar values at 95 ± 10 g dry cell/L bed volume. Since we have a small cell sendimentation zone near the top of the tower for cell recycling, the cell densities of well mixed regions were also found to be invarient with respect to different operating conditions. The measured cell density was around 60 ± 5 g dry cell/L liquid. Values of empirical constants (D_a, α, β) that best fit the experimental data are shown in Table 1. The results of curve fitting are shown in Fig. 3a through Fig. 4d.

Simulation of the Concentration Profile

Equation (1) was solved as mentioned above. The simulation was done by first solving Eq. (1) assuming that the whole column is in a packed bed form. The generated sugar concentration profiles were then subjected to the constraint of either nutrient limitation or hydrodynamic limitations:

Nutrient Limitation

When the height of the packed bed region falls under the nutrient limitation condition, the critical substrate level (at the top of the packed bed region) is independent of dilution rate and height of the packed bed region (7) (Fig. 2). Although the mechanism of cell aggregation is not yet understood, it is known that many factors (e.g., pH, ions, proteins, and so on) may affect the aggregation of cells. However, in this study, sugar

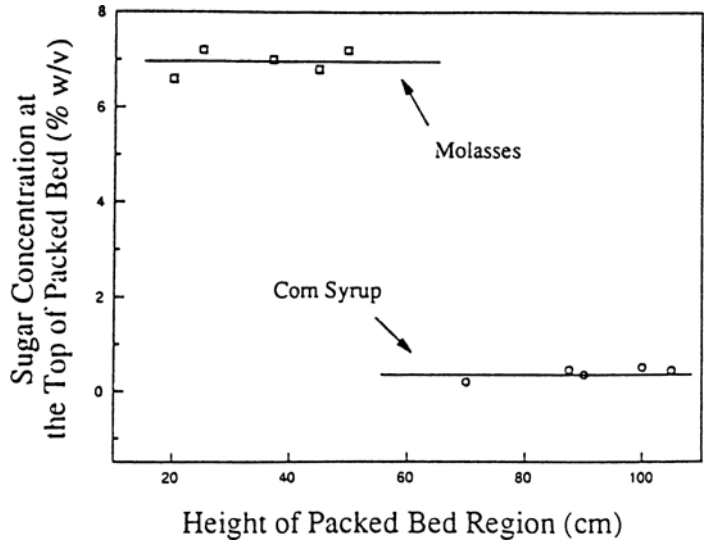

Fig. 2. Sugar conc. at the top of the packed bed region. Feed: corn syrup (15% w/v sugar); molasses (12% w/v sugar).

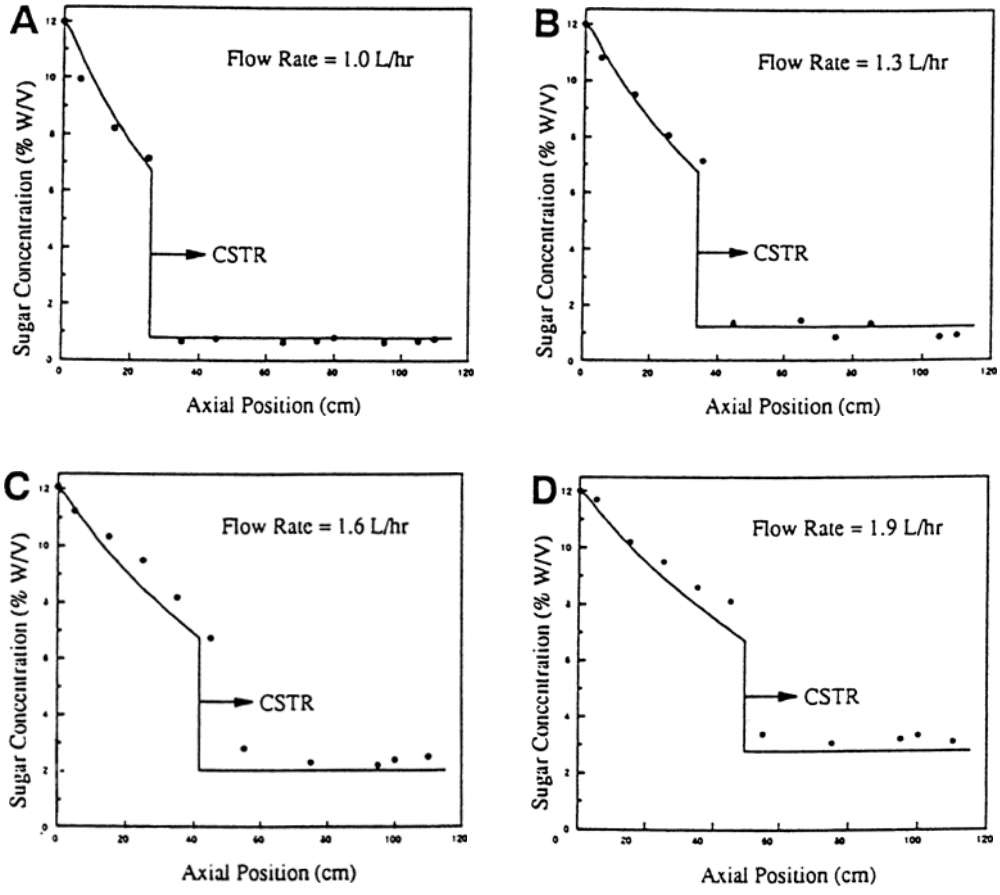

Fig. 3. Experimental and predicted sugar concentration. Profile of sugarcane molasses fermentation.

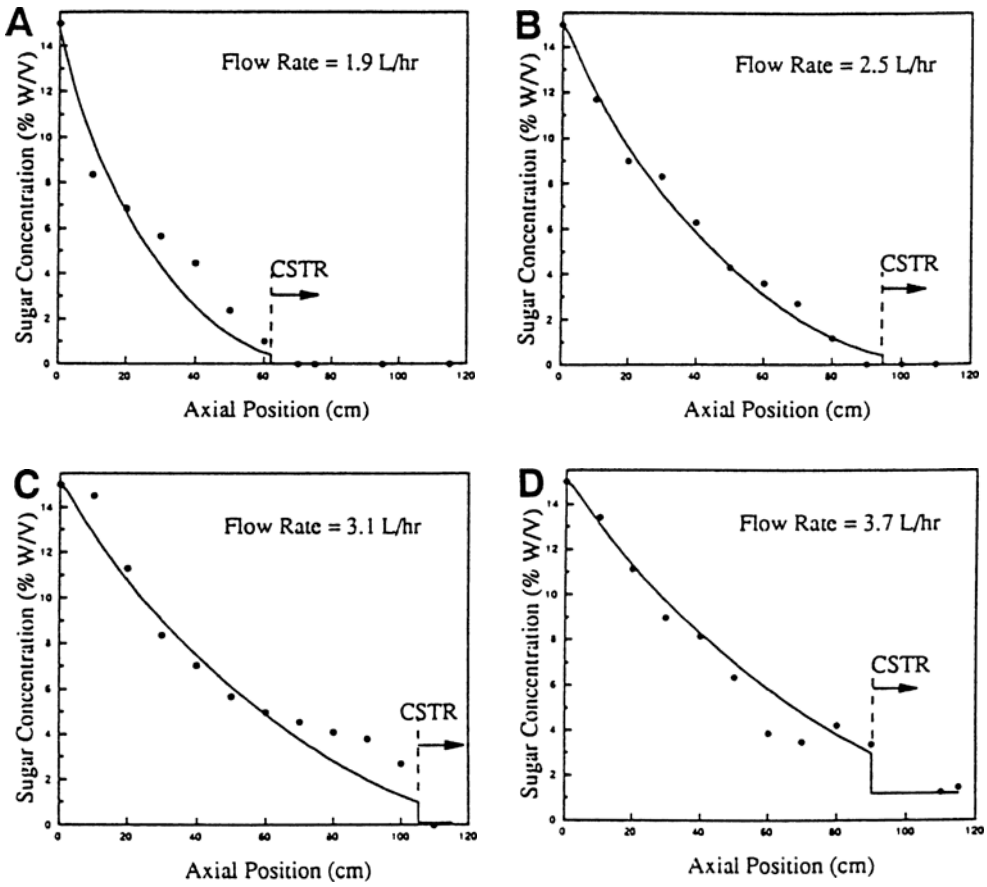

Fig. 4. Experimental and predicted sugar concentration. Profile of corn syrup fermentation.

concentration was found to be an apparent factor that can serve as an indication of the point where cell aggregates disintegrate. When sugar concentration dropped below this critical substrate level, cell aggregates disintegrated into smaller aggregates (<0.3 mm). When molasses was used, this nutrient limitation corresponds to a higher sugar concentration (about 6.7% w/v), because of the presence of inhibitory compounds (*17,18*). When corn syrup was used, this nutrient limitation corresponded to a lower sugar concentration (about 0.4% w/v).

After Eq. (1) was solved, a solution that represents the sugar concentration profile across the whole packed bed column was generated. The obtained sugar concentration profile was cut at the critical sugar level (S_c) (Fig. 2), at which nutrient limitation occurs. It was observed that on the top of the packed bed region, small cell aggregates (<0.3 mm) were well mixed by the upgoing gas (CO_2) and liquid. Figures 3a–d and 4a and b also show that at axial position higher than the point where nutrient

limitation occurs, the sugar concentration profile was down to a lower constant level. Both observation and experimental data on these figures indicate that the region above the packed bed region behaves like a CSTR. This region is therefore simulated by an ideal CSTR.

There is a clear boundary between the packed bed region and the well-mixed region during fermentation (Fig. 1). The cell aggregates in the two regions are significantly different in particle size (2–3 mm in the packed bed region and <0.3 mm in the well-mixed region). In Figs. 3a through 4b, experimental data show that the sugar concentration dropped from the critical level of nutrient limitation to a lower constant level within a distance of less than 10 cm. The observation and the measured sugar concentration profiles indicate that the transition of the fermentor from a packed bed reactor to a CSTR is very short (<10 cm). Therefore, it is assumed that the difference between this transition zone (from packed bed region to mixed region) and a CSTR will not affect appreciably the final productivity if this transition zone is treated as part of the CSTR.

For reasons mentioned above, the critical sugar concentration of nutrient limitation at the top of the packed bed region is treated as the input sugar concentration of the CSTR region. Since gas (CO_2) is flowing through the CSTR region at a high flow rate that will cause significant gas holdup in this region, Eqs. (10) and (11) were solved simultaneously for the conversion in the CSTR region by taking into account the gas holdup in this region. The true volume of the CSTR region should be the total volume of the well-mixed region subtracting the volume of the gas holdup. After Eqs. (9) and (10) were solved for the conversion in the CSTR region, a vertical straight line was drawn from the critical sugar concentration of nutrient limitation to the sugar concentration in the well mixed region (CSTR) to describe the behavior of an ideal CSTR. The difference between the short transition zone (from packed bed region to well-mixed region) and the CSTR zone was negligible. The results are shown in Figs. 3a through 4b.

Hydrodynamic Limitation

When sugar concentration drops with increasing axial position, the flow rate of carbon dioxide increases. If before the criteria of nutrient limitation is reached, the flow rate of carbon dioxide increases to a point where the cell aggregates begin to fluidize, hydrodynamic limitation will be the limiting factor for the height of the packed bed region.

Hydrodynamic limitations occurs when the total superficial fluid (carbon dioxide + liquid) velocity is higher than the minimum fluidization velocity of the yeast aggregates (7). At this point the aggregates will be fluidized, hence limits the height of the packed bed region, thus the performance of the whole fermentor. The amount of carbon dioxide flowing through different axial positions was estimated by assuming that for

every mole of ethanol produced, there is one mole of carbon dioxide generated. The carbon dioxide flow rate was then related to sugar consumption rate (Eq. (5)). The total superficial fluid velocity can therefore be monitored along the axial position given the estimated sugar concentration profile.

Among many models for fluidization, Begovich and Watson's model (*19*) gives best estimate of minimum fluidization velocity, which can also be used to estimate the point of hydrodynamic limitation. According to the calculation by the equation of Begovich and Watson (*19*), yeast cell aggregates of 2.5 mm in diameter with a bulk density of 1.26 g/cm^3 (specific gravity of the cell pellets) will begin to be fluidized at a total superficial fluid (carbon dioxide+liquid) velocity of 97 cm/min.

When the sugar concentration dropped from 15% (W/V) to about 1% (W/V) at an axial position of 105 cm, the carbon dioxide flow rate was about 1917 cm^3/min (Fig. 4c). The total fluid flow rate (CO_2 +liquid) is approximately 1969 cm^3/min. Therefore, the superficial velocity of the total fluid at that point reached a value of 97 cm/min. This is the point where with sugar concentration, at about 1% w/v (at an axial position of 105 cm), cell aggregates start to be fluidized by the upgoing fluid (CO_2 and liquid). The sugar concentration at the top of the packed bed region (1% w/v) was treated as the input sugar concentration of the CSTR region. Theoretically, Eq. (1) should be able to describe the CSTR region when the dispersion coefficient is large enough (*11*). However, in this case, huge amount of disintegrated small cell aggregates (<0.3 mm) was observed to dominate the well mixed region. Therefore, the well mixed region must be treated separately as in the case of nutrient limitation. The well-mixed region is treated as an ideal CSTR and the result is shown in Fig. 4c. A higher medium flow rate was simulated in the same manner with the same criteria of mimimum fluidization. The result is shown in Fig. 4d.

The simulation results of the concentration profiles (Figs. 3a through 4d) are close to those of the experimental data. However, in both cases (nutrient limitation or hydrodynamic limitation), this model was not able to tell what was happening in the transition zone.

Bed Height Prediction

The height of the packed bed region is limited by either nutrient limitation or hydrodynamic limitation, as mentioned earlier. Once the sugar concentration profiles generated for either nutrient limitation or hydrodynamic limitation were obtained, the height of the packed bed region could be estimated. The vertical lines in Figs. 3a through 4b were drawn at positions where nutrient limitations occurred. This axial position is the height of the packed bed region under corresponding operation condition. In Figs. 4c and d, the vertical lines were drawn at positions where hydrodynamic limitation occurred. This axial position is the height of the packed

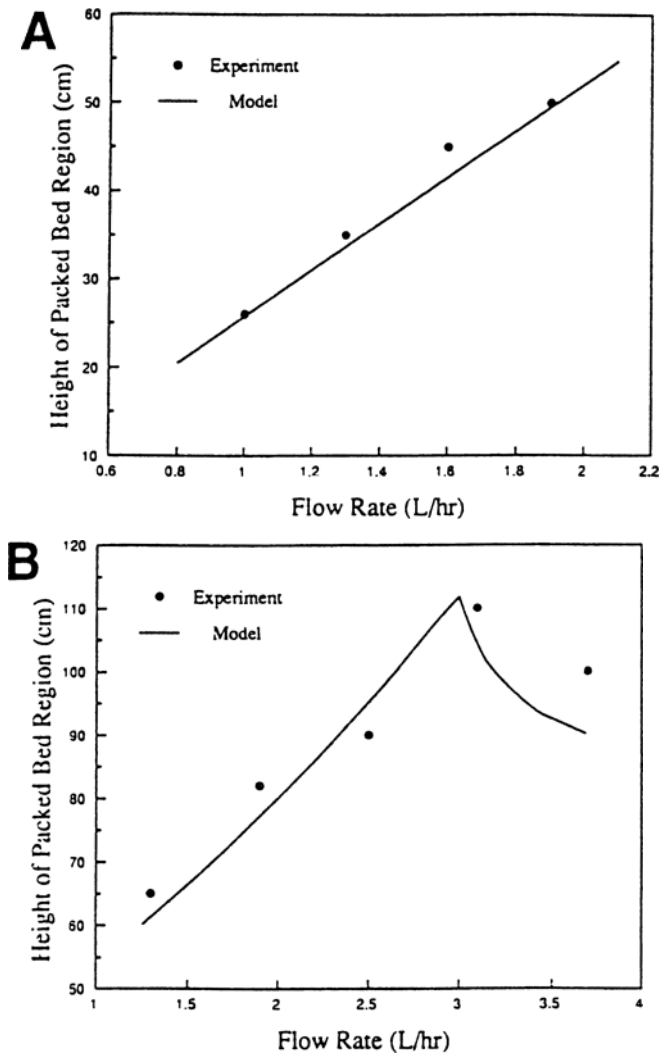

Fig. 5. Experimental and predicted height of packed bed region. (a) molasses fermentation; (b) corn syrup fermentation.

bed region when hydrodynamic limitation is limiting the bed height under the corresponding operation condition.

Figure 5a shows the relationship between medium flow rate and the height of the packed bed region in the case of molasses fermentation. Figure 5b demonstrates this relationship of corn syrup fermentation. Solid lines in Figs. 5a and b are the height of the packed bed region predicted by the model as described above, whereas solid circles are observed values. As we can see in these two figures, bed height increases as dilution rate increases when the column is under nutrient limitation. However, the bed height decreased as medium flow rate increased when hydrodynamic

limitations occurs. When corn syrup was used as the substrate, the height of the packed bed region increased with increasing medium flow rate until a medium flow rate of about 2.9 L/h (Fig. 5b) was attained. The flow rates of generated carbon dioxide and liquid are high enough to fluidize the cell aggregates. If the medium flow rate is increased further, the height of the packed bed region begins to decrease. This decrease of bed height is caused by generation of carbon dioxide at a greater rate. In the case of molasses fermentation, the fermentation rate is slower (Table 1). Hydrodynamic limitation is not easy to obtain within practical range of operation.

Productivity Prediction

With this model, the ethanol concentration at the top of the tower fermentor and the productivity of this fermentor can be easily calculated. Figures 6a and b show the predicted ethanol concentrations and productivities, and their comparison with the experimental results. From Figs. 6a and 6b, we can see that the measured ethanol concentrations were all higher than our predictions. This may be caused by the condensation of the ethanol carried by air bubbles to the top of the tower. The prediction will be better if we consider the local evaporation of ethanol and its condensation at the top of the fermentor.

CONCLUSION

An ethanolic tower fermentor using self-aggregating yeast consists of a distinct packed bed region and a well mixed region. The height of the packed bed region was found to be affected by nutrient limitation and hydrodynamic limitation.

By modeling a serial connection of a packed bed reactor with variable axial dispersion and a CSTR, we are able to predict the concentration profile, the height of the packed bed region, and the productivity. This model can simulate for both molasses and corn syrup fermentation operated under a wide range of flow rates. The transition from packed bed region to well-mixed region could not be described by this model. However, the transition zone between the packed bed region and the well-mixed region was very narrow. The difference between the transition zone and a CSTR did not appreciably affect the final conversion. This model can be applied to different substrates under nutrient limitation and hydrodynamic limitation conditions.

ACKNOWLEDGMENTS

The sponsorship of Savannah Food and Industries and US Sugar Corp. was deeply appreciated.

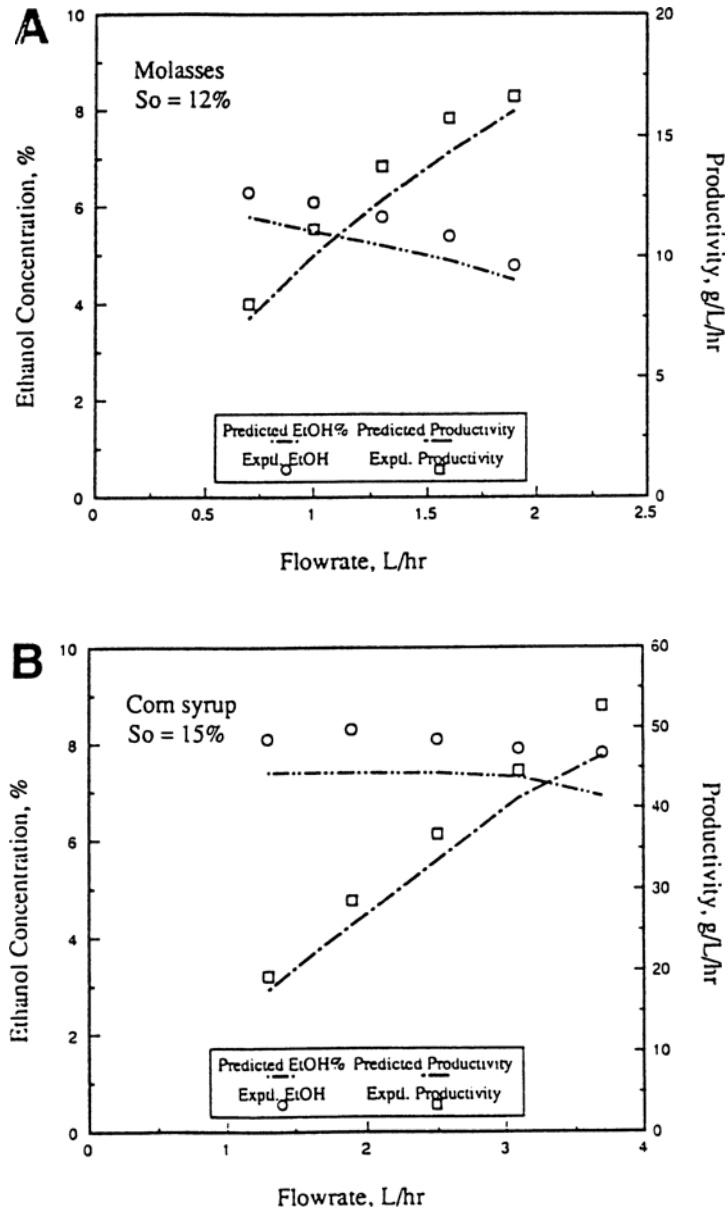

Fig. 6. Ethanol concentration and productivity when (a) molasses or (b) corn syrup was used as the substrate.

REFERENCES

1. Admassu, W. and Korus, R. (1985), *The Chem. Eng. J.* **31,** 1.
2. Bu'lock, J. D., Comberbach, D. M., and Ghommich, C. (1984), *Chem. Eng. J.* **29,** 9.

3. Hamamci, H. and Ryn, D. Y. (1988), *Appl. Microbiol. Biotechnol.* **28,** 515.
4. Jones, S. T., Korus, R. A., Admassu, W., and Heimsch, R. C. (1984), *Biotech. Bioeng.* **26,** 742.
5. Prince, I. G. and Bardord, J. P. (1982), *Biotech. Lett.* **4(7),** 469.
6. Levenspiel, O. (1972), *Chemical Reaction Engineering,* 2nd ed., Wiley, NY, Ch.6.
7. Chen, C. S., Chan, E., Gong, C. S., and Chen, L. F. (1991), *Appl. Biochem. Biotech.* **28/29,** 719.
8. Chen, L. F. and Gong, C. S. (1985), *Biotechnol. Bioeng.* **14,** 257.
9. Chen, L. F. and Gong, C. S. (1986), *Appl. Microbiol. Biotechnol.* **25,** 208.
10. Kida, K., Asano, S., Yamadaki, M., Iwasaki, K., Yamaguchi, T., and Sonoda, Y. (1990), *J. Ferment. Bioeng.* **69(1),** 39.
11. Perterson, J. N. and Davison, B. H. (1991), *Appl. Biochem. Biotech.* **28/29,** 685.
12. Ascher, U., Christiansen, J., and Russel, R. D. (1979), *Math. Comput.* **33,** 659.
13. Ascher, U., Christiansen, J., and Russel, R. D. (1981), *ACM TOMS* **7,** 209.
14. Mersmann, A. (1978), *Ger. Chem. Eng.* **1,** 1.
15. Luong, J. H. T. (1985), *Biotechnol. Bioeng.* **27,** 280.
16. Lee, K. J. and Rogers, P. L. (1983), *Chem. Eng. J.* **27,** 31.
17. Leonard, R. H. and Hainy, G. J. (1945), *Ind. Eng. Chem.* **37,** 390.
18. Maiorella, B. L., Blanch, H. W., and Wilke, C. R. (1984), *Biotech. Bioeng.* **26,** 1155.
19. Begovich, J. M. and Watson, J. S. (1978), *Fluidization,* Davidson, J. F. and Keairns, D. L., eds., Cambridge University Press, Cambridge, UK, pp. 190–195.